

The cluster environments of powerful radio-loud and radio-quiet AGN

R.J. McLure¹ & J.S. Dunlop²

¹*Nuclear and Astrophysics Laboratory, University of Oxford, Keble Road, Oxford, OX1 3RH*

²*Institute for Astronomy, University of Edinburgh, Blackford Hill, Edinburgh, 3H9 3HJ*

Submitted for publication in MNRAS

ABSTRACT

The spatial clustering amplitude (B_{gg}) is determined for a sample of 44 powerful AGN at $z \simeq 0.2$. No significant difference is detected in the richness of the cluster environments of the radio-loud and radio-quiet sub-samples, both of which typically inhabit environments as rich as Abell Class $\simeq 0$. Comparison with radio luminosity-matched samples from Hill & Lilly (1991) and Wold et al. (2000a) suggests that there is no epoch-dependent change in environment richness out to at least $z \geq 0.5$ for either radio galaxies or radio quasars. Comparison with the APM cluster survey shows that, contrary to current folklore, powerful AGN do not avoid rich clusters, but rather display a spread in cluster environment which is perfectly consistent with being drawn at random from the massive elliptical population. Finally, we argue that virtually all Abell class $\simeq 0$ clusters contained an active galaxy during the epoch of peak quasar activity at $z \sim 2.5$.

Key words: galaxies: clustering – galaxies: active – quasars: general

1 INTRODUCTION

The cluster environments of active galactic nuclei (AGN) provide important information for improving our understanding of several aspects of the AGN phenomenon. Over the last fifteen years a considerable amount of effort has been invested in studying the environments of several different types of AGN, including : radio-quiet and radio-loud quasars (eg. Yee & Green 1984, 1987, Smith, Boyle & Maddox 1995, 2000, Hall & Green 1998), radio galaxies (Prestage & Peacock 1988, 1989, Hill & Lilly 1991), BLLacs (Wurtz et al. 1997) and Seyfert galaxies (de Robertis & Yee 1998). In addition to its potential for shedding light on the processes by which dormant black holes are triggered into AGN, the study of clustering environments is an invaluable test of the viability of proposed unification schemes (eg. Wurtz et al. 1997) and models of quasar evolution (eg. Ellingson, Green & Yee 1991). In this paper we use HST images to study the immediate environments of AGN drawn from well-matched samples of powerful radio galaxies (RG), radio-loud quasars (RLQ) and radio-quiet quasars (RQQ) at $z = 0.2$ to explore what constraints can be placed on the origin of radio loudness, the viability of radio loud unification, and the physical origin of the dramatic evolution of the quasar population between $z = 2.0$ and the present day.

Several authors have reported a difference in the richness of clustering around radio-loud and radio-quiet quasars (eg. Yee & Green 1984, 1987, Ellingson, Green & Yee 1991).

These studies have shown that, with substantial overlap, low to moderate redshift radio-loud quasars are found in Abell 0/1 clusters, while radio-quiet quasars rarely inhabit clusters as rich as Abell 0. This apparent change in quasar environment with radio-power was at least consistent with the traditional picture in which RLQs have elliptical host galaxies, and are therefore preferentially found in clusters, while RQQs inhabit the poorer environments associated with lower luminosity disc-dominated Seyfert galaxies.

However, the results of our own HST host galaxy imaging programme (McLure et al. 1999, Dunlop et al. 2000), together with other recent HST and ground-based studies (eg. Hooper et al. 1997, Boyce et al. 1998, Bahcall et al. 1997, Schade et al. 2000) show that, at the very least, a significant fraction of the RQQ population are located in elliptical host galaxies. In fact, the results of our own study lead to the conclusion that all objects which could be classified as *true* quasars (i.e. $M_V < -23$) will have bulge-dominated host galaxies. In Section 4.1 we therefore examine the question of whether our target RQQs and RLQs, drawn from samples well matched in terms of AGN luminosity, are actually occupying significantly different cluster environments.

The other question investigated in this paper is that of the evolution of the cluster environments of powerful, radio-loud AGN. With respect to radio galaxies, it was shown by Prestage & Peacock (1988, 1989) that at low z the environments of powerful FR II sources are poorer than their FR I counterparts, although the substantial overlap between the

arXiv:astro-ph/0007219v1 16 Jul 2000

two populations led Prestage & Peacock to conclude that environment did not solely determine radio luminosity. In contrast, at higher redshifts, $z \simeq 0.5$, both Yates, Miller & Peacock (1989) and Hill & Lilly (1991) found that radio galaxies inhabited richer clusters than at low redshift, leading Hill & Lilly to conclude that the cluster environments of radio galaxies were epoch-dependent. Similar conclusions were reached by Ellingson, Green & Yee (1991) from their study of the environments of RLQs. Ellingson et al. found that the environments of RLQs also become richer at $z > 0.6$, although the existence of this epoch-dependence has recently been questioned by Wold et al. (2000a).

In contrast to what might be expected from the results outlined above, the raw HST images from our sample of RGs and RLQs (Dunlop et al. 2000) show many of the objects to be apparently residing in clusters of moderate richness, an impression which is confirmed by the analysis presented in Section 4. Motivated by this, in Sections 5.1 & 5.2 we present a comparison between the cluster results for our RG and RLQ samples with those for optical and radio luminosity-matched sub-samples of the objects studied by Hill & Lilly (1991) and Wold et al. (2000a), in order to critically re-examine the evidence that RGs and RLQs inhabit environments which are a function of cosmic epoch. In Section 6 we investigate whether there is any evidence in our data for a link between AGN properties and the large-scale environments of their hosts. Finally, in Section 7 we compare the distribution of cluster richness determined for our sample with that of the APM cluster survey (Dalton et al. 1997, Croft et al. 1997) in light of the constraint imposed by our host galaxy study that only galaxies with $M_R \leq -23$ are capable of producing powerful AGN. Unless otherwise specified all cosmological calculations performed in this paper assume a cosmology of $H_0 = 50$, $q_0 = 0.5$ and $\Lambda = 0$.

2 THE SAMPLE

The low-redshift sample studied in this paper comprises 44 objects and is a combination of that investigated in our HST study of $z \simeq 0.2$ AGN host galaxies (McLure et al. 1999, Dunlop et al. 2000), with data of similar quality from the HST archive. The sample investigated in our host-galaxy programme consisted of 33 objects, divided into three sub-samples of 10 radio galaxies (RG), 10 radio-loud quasars (RLQ) and 13 radio-quiet quasars (RQQ). The unique feature of this sample is that the two quasar sub-samples were originally chosen to be matched in terms of their distribution in the optical luminosity-redshift plane ($M_V - z$) (Dunlop et al. 1993), with the RG and RLQ sub-samples matched in both the radio power-redshift plane ($P_{5GHz} - z$), and the radio power-spectral index plane ($P_{5GHz} - \alpha$) (Taylor et al. 1996). Although the selection criteria used in choosing these samples were designed to determine the role played by host galaxies in the radio-loudness dichotomy and radio-loud unification, they are equally valid for investigating the nature of their respective cluster environments. One of the objects from this sample, the RQQ 1549+203, has however been excluded from this analysis due to the known presence of a foreground cluster (Stocke et al. 1983). In order to increase the numbers of objects studied we have also included in our sample 12 quasars from the HST study of Bahcall et

al. (1997) which were not included in our host galaxy study. Although image saturation and emission line contamination make the Bahcall et al. data flawed with respect to detailed host galaxy analysis, these problems are not a concern for an environmental study. The data for these objects (3 RLQs & 9 RQQs) is of practically identical depth to our own and, with the exception of 3C273, falls in the same region of the $M_V - z$ plane.

2.1 Observations and data reduction

The observations for all 44 objects considered in this paper were taken with the HST Wide-Field and Planetary Camera 2 (WFPC2). The observations for the 33 objects from our $z = 0.2$ host galaxy study utilised the F675W filter, which closely approximates the standard Cousins *R*-band (Holtzman et al. 1995), while the data for the objects from the Bahcall et al. sample were taken with the F606W (Wide *V*) filter. Both data sets were imaged on the wide-field chips of WFPC2 (WF2 for the F675W data and WF3 for the F606W data) and have a plate-scale of $0.1''/\text{pix}$.

The basic data reduction (bias removal & flat-fielding) was performed by the HST pipeline. Subsequently, the individual exposures of each source ($3 \times 600\text{s}$ for the F675W data and typically $1100\text{s}+600\text{s}$ for the F606W data) were then combined and cleaned of cosmic rays using standard IRAF tasks. The signal-to-noise levels in the final deep images correspond to a Cousins *R*-band 1σ sensitivity limit of $\mu_R \simeq 26.7 \text{ mag arcsec}^{-2}$, where the conversion from F606W to Cousins *R*-band for the Bahcall et al. data assumes a typical colour for a $z = 0.2$ E/Sab galaxy of $R_c = 606 - 0.3$ (Fukugita et al. 1995).

3 DETERMINING CLUSTER RICHNESS

The method adopted in this study for quantifying the richness of the AGN environments was to determine their respective spatial clustering amplitudes (B_{gq}) (Longair & Seldner 1979). This is a standard technique which, although originally designed to investigate clustering around radio galaxies, has subsequently been successfully applied to the environments of a wide variety of active and inactive galaxies (eg. Yee & López-Cruz 1999, Ellingson, Yee & Green 1991, Prestage & Peacock 1988). A detailed description of the derivation of B_{gq} is given in Longair & Seldner (1979) and consequently only a brief outline is provided here. The first stage in the calculation is the determination of the angular correlation function, defined as :

$$n(\theta) \delta\Omega = N_g [1 + w(\theta)] \delta\Omega \quad (1)$$

where

$$w(\theta) = A_{gq} \theta^{1-\gamma} \quad (2)$$

and A_{gq} quantifies the excess in the number of galaxies in the vicinity of the source as compared to the expected background contribution N_g . Provided that $\theta \ll 1$ the value of A_{gq} can be directly calculated from the data using the expression:

$$A_{gq} = \left[\frac{N_t}{N_b} - 1 \right] \left(\frac{3-\gamma}{2} \right) \theta^{\gamma-1} \quad (3)$$

where N_i is the total number of galaxies counted within a radius of θ radians from the target (excluding the target itself), and N_b is the expected number of background galaxies within the same radius. In order to directly compare the clustering around objects which cover a range of redshifts it is then necessary to de-project this angular correlation into its spatial equivalent which is defined by:

$$n(r) \delta V = \rho_g [1 + \epsilon(r)] \delta V \quad (4)$$

where

$$\epsilon(r) = B_{gq} r^{-\gamma} \quad (5)$$

and B_{gq} is the desired spatial clustering amplitude. By invoking the simplifying assumption that the clustering of galaxies is spherically symmetric around the central object it can be shown (Longair & Seldner 1979) that the spatial and angular clustering amplitudes are related by the expression:

$$B_{gq} = \frac{A_{gq} N_g}{I_\gamma \phi(z)} \left[\frac{D}{1+z} \right]^{\gamma-3} \quad (6)$$

where D is the effective angular diameter distance to the target and $\phi(z)$ is the integrated field-galaxy luminosity function at the redshift of the target. The quantity I_γ is a constant which has a value of 3.78 for the canonical field-galaxy value of $\gamma = 1.77$ (Groth & Peebles 1977).

For a galaxy appearing on the same WF CCD as one of the AGN in this sample to be counted as a possible cluster member it had to satisfy two criteria. Firstly, its projected distance from the central object had to be less than the counting radius; defined as the distance of the central object from the nearest edge of the CCD. At the sample median redshift of $z=0.2$ this radius corresponds to a projected metric radius of typically 180 kpc. Although this is undoubtedly a small counting radius compared to the usual 500 kpc or 1 Mpc counting radii adopted in most cluster studies, provided that the clustering of galaxies around the AGN does have a slope of $\gamma = 1.77$, the restriction of only having information of the central regions of the clusters should not prevent a reliable determination of the enhancement of associated galaxies relative to the field population. Indeed, as will be discussed in Section 3.2, there is good evidence that the clustering around the AGN studied here does follow the expected slope of $\gamma = 1.77$, at least on average. Furthermore, in their recent study of low- z Abell clusters, Yee & López-Cruz (1999) found that reducing the counting radius from 1 Mpc to 200 kpc only altered the spatial clustering amplitude determination at the 10 percent level.

The second selection criterion was that galaxies had to lie in the magnitude interval $m_* - 1 \rightarrow m_* + 2$, where m_* is the apparent magnitude corresponding to M_* at the AGN redshift. This magnitude interval is a compromise which is designed to include those cluster galaxies which contain the majority of the cluster mass. The faint limit of $m_* + 2$ should probe deep enough into the cluster luminosity function to be sensitive to any enhancements in galaxy density, without risking the possibility of missing clusters due to the background galaxy counts rising more rapidly than the faint-end of the cluster luminosity function at $m > m_* + 2$. The bright limit of $m_* - 1$ is set to avoid problems associated with small number statistics, although relaxation of this limit to $m_* - 3$ has a negligible effect on the results presented in Section 4. An additional advantage with this choice of magnitude in-

z	ϕ/Mpc^{-3}	M_R^*	α
0.00 \rightarrow 0.20	0.0023	-22.20	1.00
0.20 \rightarrow 0.50	0.0034	-22.32	1.03
0.50 \rightarrow 0.75	0.0078	-22.11	0.50
0.75 \rightarrow 2.00	0.0068	-22.52	1.28

Table 1. The Schechter luminosity function parameters used to predict the background galaxy counts. Column 1 lists the four redshift bins adopted. The parameters for the lowest redshift bin have been taken from Yee & López-Cruz (1999). The parameters in the other three redshift bins have been taken from Lilly et al. (1995) with a conversion of M_* deduced assuming typical colours of $B - B_{AB} = 0.17$ (Metcalfe et al. 1991) and $R - B = 1.45$ (Fukugita et al. 1995).

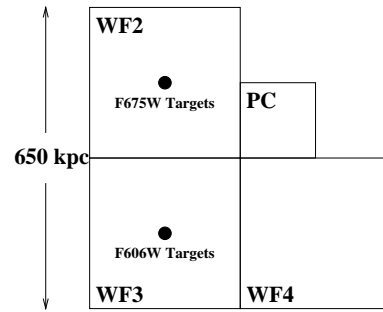


Figure 1. A schematic of the Wide Field and Planetary Camera 2 showing the spatial coverage at the median redshift of $z = 0.2$. The 32 objects imaged during the AGN host galaxy study of McLure et al. (1999) and Dunlop et al. (2000) are centred on WF2. The 12 objects included from the sample of Bahcall et al. (1997) were imaged on WF3. The extra separation of WF2 and WF4 allowed the distribution of background galaxies and the slope of the correlation function to be investigated (Section 3).

terval is that, due to the host galaxies of the AGN studied in our HST imaging programme having average luminosities one magnitude brighter than M_* (Dunlop et al. 2000), this interval typically corresponds to the $m_g \rightarrow m_g + 3$ range adopted for the Abell-type calculation of cluster richness around $z \simeq 0.5$ radio galaxies by Hill & Lilly (1991). The comparison presented in Section 5.1 of the clustering around the $z \simeq 0.2$ radio galaxies studied here, with the results obtained by Hill & Lilly (1991), can consequently be performed in a more transparent manner.

3.1 Galaxy counts and the luminosity function

A crucial element in the calculation of the spatial clustering amplitude is the form of the luminosity function used in the normalization of equation 6. Given that the derivation of equation 6 is dependent on the assumption that the observed background galaxy counts can be predicted from integrating the galaxy luminosity function along the line of sight, it is essential that the luminosity function chosen should at least be consistent with the background counts. In order to ensure this we have adopted a similar approach to that employed by Wold et al. (2000a), by considering the form of the luminosity function in four redshift bins $z=(0.0,$

0.2), (0.2, 0.5), (0.5, 0.75) & (0.75, 2.0). The Schechter function parameters of the four luminosity functions are listed in Table 1. In the lowest redshift bin we have adopted the luminosity function determined by Yee & López-Cruz (1999) from their *R*-band study of Abell clusters in the redshift range $0.02 < z < 0.18$. The characteristic magnitude and faint-end slope of this Schechter function are nearly identical to those determined for the field-galaxy population by Loveday et al. (1992), but with a normalization some 30% higher. Due to the fact that the Loveday et al. determination from the Stromlo-APM survey is dominated by objects with $z < 0.1$, it was felt that the Yee & López-Cruz luminosity function was a fairer representation of the $z \simeq 0.2$ galaxy population. The adoption of the higher normalization also has the advantage that we are correspondingly less likely to be overestimating the spatial clustering amplitudes. In the three highest redshift bins the parameters are taken from Lilly et al. (1995), with the appropriate conversion of the characteristic magnitudes from the M_{AB} system to the Cousins *R*-band (see Table 1). The predicted number counts in a particular magnitude range (m_1, m_2) were then calculated by integrating the following function:

$$\int_{z=0}^{z=2} \int_{m_1}^{m_2} \phi(m, z) \delta m \left(\frac{\delta V}{\delta z} \right) \delta z \quad (7)$$

where the limiting redshift of $z = 2$ was chosen since, in the magnitude range investigated here ($R < 24$), the contribution from background galaxies at $z \geq 2$ is negligible. A comparison between the predicted and measured galaxy counts for both the target (WF2+WF3) and control CCDs (WF4) is shown in Fig 2. It can be seen that the predicted background galaxy counts (left panel) agree well with those measured in the magnitude range ($21 < R < 23$), where the control chips should be relatively unaffected by contamination from cluster members. However, in the magnitude range $18.5 < R < 20.5$ there is an excess of detected background galaxies over that predicted, as expected given that at our median redshift of $z = 0.2$ this range corresponds to $M_* \rightarrow M_* + 2$. The predicted background counts are in good agreement with those determined by both Yee & López-Cruz (1999) and Metcalfe et al. (1991) and were subsequently used to remove the background contribution in the calculations of the spatial clustering amplitude. The comparison between the predicted background counts and the counts from the AGN target CCDs shows qualitatively that inside a radius of $\simeq 200$ kpc we are clearly detecting a large excess of cluster galaxies.

3.2 The slope of the correlation function

The usual procedure when determining the richness of a cluster environment via its spatial clustering amplitude is to assume that the slope of the two-point correlation function has the canonical value of $\gamma = 1.77$ (Groth & Peebles 1977). Here we investigate whether this is in fact a reasonable assumption for the objects in this sample. As a result of the relative positions of the WF2 and WF4 CCDs on the WFPC2 (see Fig 1) it is possible to perform galaxy ring counts out to a projected radius of $\simeq 800$ kpc for the 32 objects imaged through the F675W filter, under the assumption of spherical symmetry. Fig 3 shows the average radial

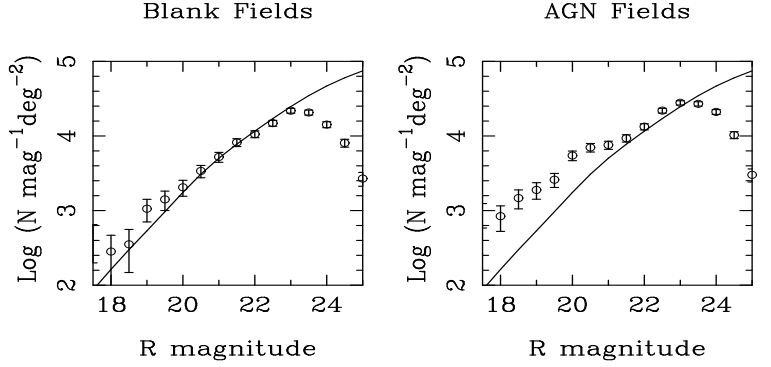


Figure 2. The left-hand panel shows the background galaxy number counts from the 32 WF4 observations from McLure et al. (1999) and Dunlop et al. (2000), at an average separation from the target AGN of $\simeq 500$ kpc. The solid line is the predicted number counts from integrating the galaxy luminosity function along the line of sight (see text for discussion). The right-hand panel shows the galaxy counts from the target WF chips of all 44 objects at a separation of ≤ 200 kpc. A clear excess of galaxies is obvious at $R < 23$.

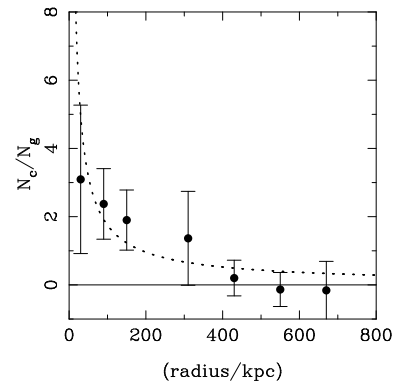


Figure 3. Radial profile showing the average ratio of excess cluster galaxies (N_c) to background galaxies (N_g). The width of the bins changes from 60 kpc to 120 kpc at a radius of 220 kpc in order to maintain comparable signal-to-noise. Also shown is the best-fit power-law correlation function (dotted line). The best fit value of γ is $1.88^{+0.10}_{-0.09}$ where the errors refer to the $\Delta\chi^2 - \Delta\chi^2_{min} = 1$ confidence limit.

profile of the ratio of cluster galaxies to background galaxies (N_c/N_g) measured in metric aperture bins. In order to keep the signal-to-noise level of the bins approximately constant their width is increased from 60 kpc to 120 kpc at a radius of 200 kpc. The dotted line in Fig 3 shows the minimum χ^2 fit for the angular correlation function, as defined in equation 2, which has a value of $\gamma = 1.88^{+0.10}_{-0.09}$. It appears therefore that, at least on average, the form of the correlation function for the objects in this sample is consistent with the standard value of $\gamma = 1.77$. Consequently, we adopt this standard value in our calculation of the spatial clustering amplitudes in order to allow easy comparison with results in the literature.

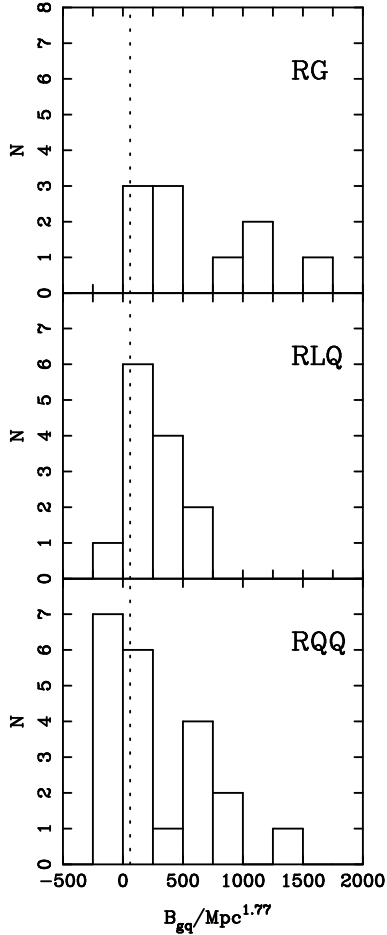


Figure 4. Histograms showing the distribution of clustering amplitudes displayed by the three sub-samples. Also shown in the approximate level of the clustering amplitudes of field galaxies (dotted line), here taken as $B_{gq} = 60$

Sample	N	$\langle B_{gq} \rangle$	Median
All	44	365 ± 62	241
RG	10	575 ± 165	321
RLQ	13	267 ± 51	247
RQQ	21	326 ± 94	209

Table 2. Summary of the spatial clustering amplitude results. Column two details the number of objects in each sub-sample.

4 RESULTS

The results of the B_{gq} calculations for the three sub-samples are listed in column 6 of Table 3 and are shown graphically in Figs 4 & 5. In this section we discuss the results for the separate sub-samples in the context of the results of our host galaxy study (McLure et al. 1999, Dunlop et al. 2000) and previous studies of similar objects from the literature. In Sections 5.1 & 5.2 we proceed to perform a more detailed comparison between our results and those obtained by Hill & Lilly (1991) and Wold et al. (2000a) at higher redshift.

4.1 Do RLQs reside in richer environments than RQQs?

The clustering results for the two quasar sub-samples shown in Tables 2 & 3 indicate that there is no significant difference in the richness of the cluster environments of the RQQs and RLQs studied here. It can be seen from Table 2 that the two sub-samples display mean and median clustering amplitudes which are statistically consistent, with the Kolmogorov-Smirnov (KS) test returning a significance level of only $p=0.54$.

The finding that RLQs inhabit environments with spatial clustering amplitudes of the order $\sim 200 \rightarrow 300 \text{ Mpc}^{1.77}$ is in good agreement with previous studies. For example, the large-scale study of Ellingson, Yee & Green (1991) found that at $z < 0.4$ the average clustering amplitude of RLQs was $210 \pm 70 \text{ Mpc}^{1.77}$. Moreover, the clustering study performed by Fisher et al. (1996) using the HST data for the 20 quasars in the Bahcall et al. (1997) sample (all of which are common to the 44 object sample studied in this paper) found the 6 RLQs in that sample to have an average clustering amplitude of $\simeq 256 \pm 55 \text{ Mpc}^{1.77}$.

In contrast, the finding that the environments of RQQs are indistinguishable from those of RLQs is not in general agreement with the literature, with the majority of previous studies concluding that RQQs tend to inhabit poorer environments. For example, the studies of both Ellingson, Yee & Green (1991) and Smith, Boyle & Maddox (1995) find the clustering around RQQs at $z < 0.3$ to be perfectly consistent with that of field galaxies, $B_{gq}/B_{gg} = 1.0$, while in contrast even the median value found here corresponds to $B_{gq}/B_{gg} = 3.8$, taking $B_{gg} = 60$. The exact cause of this discrepancy is difficult to determine due to the large number of factors which influence the calculation of B_{gq} . One possible explanation for the disagreement between these results and those of Smith et al. is that $\simeq 80\%$ of their objects are fainter than $M_V = -23$, which could explain the detection of environments typical of Seyfert galaxies (eg. de Robertis & Yee 1998). This issue was looked at by Smith et al., who found no significant difference in their results if they divided their objects into high and low luminosity sub-samples, although this split would still have resulted in $\sim 50\%$ of the objects in the high-luminosity sub-sample being fainter than $M_V = -23$.

It is worth noting at this point that the results presented by Fisher et al. (1996) of the clustering around the quasars in the Bahcall et al. (1997) sample do agree with the results presented here. Fisher et al. found an average value of $B_{gq} = 246 \pm 68 \text{ Mpc}^{1.77}$ for Bahcall's sample of 14 RQQs, data for all of which are included in the 21 RQQs studied here. Given that both of our studies are based on HST data this obviously raises the concern that the small field of view of WFPC2 has led to an overestimate of the richness of the RQQs environments. However, there are several reasons for believing that this is not a serious issue. Firstly, as demonstrated by Fig 3, there is no real suggestion that the enhancement in associated galaxies is falling off faster than $\gamma = 1.77$. Secondly, given the good agreement between our results for the RLQ sub-sample and previous studies, the form of clustering around the RQQs would have to be substantially different from that around RLQs in order to account for the difference. Although this is undoubtedly a

possibility, it is not supported by our data, with the F675W images showing no tendency for the RQQs to have fewer associated galaxies at radii of $200 < r < 700$ kpc. It appears therefore that the similarity in environments of our RQQ and RLQ samples probably results from the close matching of the samples in the $M_V - z$ plane. This conclusion is supported by the preliminary results of Wold et al. (2000b), who also find no difference in cluster environment between their optically matched samples of RQQs and RLQs in the redshift range $0.5 < z < 0.8$.

4.2 Are the environments of RLQs and RGs consistent with unification?

With the results of our host-galaxy study showing that our RG and RLQ samples are virtually identical in terms of scalelength, luminosity, and $R - K$ colour, it was expected that their cluster environments would also be indistinguishable. The results presented in Table 3 and Fig 4 broadly confirm this expectation, although it is clear that the cluster environments of the two samples are not as similar as suggested by the optical properties of their host galaxies. The application of the KS test shows the two distributions to be distinguishable only at the 1σ level ($p = 0.25$), a difference which is clearly due to the three RGs with $B_{gq} > 1000$ Mpc^{1.77}. Considering the large errors associated with the B_{gq} calculation, and the small number statistics, perhaps the strongest statement that can be made is that these results present no problem to the orientation-based unification of RGs and RLQs due to differences in cluster environment. The possibility of a correlation between environment and radio power is investigated in Section 6

4.3 Abell classification

In this section we attempt to provide a transformation between the spatial clustering amplitudes and the traditional Abell cluster classification (Abell 1958, Abell, Corwin & Olowin 1989). Unfortunately, due to numerous sources of systematic error associated with Abell counts, the correlation between Abell class and B_{gq} has a large scatter, and a consensus on the appropriate calibration has not been reached in the literature. In their study of 47 $z < 0.2$ Abell clusters Yee & López-Cruz (1999) proposed a linear scheme whereby adjacent Abell classes are separated by $\Delta B_{gq} = 400$ Mpc^{1.77}, with a normalization such that Abell class 0 clusters have a spatial clustering amplitude of $B_{gq} = 600$ Mpc^{1.77}. Here we have chosen to classify our cluster measurements using a scheme which is identical to that proposed by Yee & López-Cruz save for a re-calibration such that Abell class 0 clusters correspond to $B_{gq} = 300$ Mpc^{1.77} (Table 4).

The main reason for this re-calibration is that, unlike the clusters of class ≥ 1 , the Abell 0 clusters studied by Yee & López-Cruz were not selected randomly, but specifically chosen as being rich. Consequently, it is almost certainly the case that a figure of $B_{gq} = 600$ Mpc^{1.77} is not representative of Abell 0 clusters as a whole. Moreover, spatial clustering amplitudes of $B_{gq} = 300$ & 700 Mpc^{1.77} for Abell classes 0 & 1 are much more representative of the findings of several previous studies (eg. Longair & Seldner 1979, Prestage

Source	z	V	M_V	P_{5GHz}	$B_{gq} \pm \Delta B_{gq}$
RG					
0230-027	0.239	19.2	-20.8	24.84	308±348
0307+169	0.256	18.8	-21.5	25.52	1067±498
0345+337	0.244	19.0	-21.9	25.45	334±364
0917+459	0.174	17.2	-22.0	25.69	1070±549
0958+291	0.185	17.3	-22.1	25.30	763±471
1215-033	0.184	18.9	-20.5	24.00	90±265
1215+013	0.118	17.0	-22.3	23.97	299±371
1330+022	0.215	18.3	-21.4	25.35	28±258
1342-016	0.167	17.8	-21.6	24.35	1593±658
2141+279	0.215	18.3	-21.4	25.17	202±313
RLQ					
0137+012	0.258	17.1	-23.9	25.26	582±413
0736+017	0.191	16.5	-23.8	25.35	67±257
1004+130	0.240	15.2	-25.7	24.94	-53±240
1020-103	0.197	16.1	-24.2	24.73	266±331
1217+023	0.240	16.5	-24.3	24.92	304±347
1226+023	0.158	12.9	-27.1	26.47	165±295
1302-102	0.286	15.2	-26.1	25.28	320±363
1545+210	0.266	16.7	-24.4	25.26	383±371
2135-147	0.200	15.5	-24.9	25.27	247±324
2141+175	0.213	15.7	-24.8	24.81	208±315
2247+140	0.237	15.3	-23.9	25.31	139±302
2349-014	0.173	15.3	-24.7	24.86	610±443
2355-082	0.210	17.5	-23.0	24.50	235±326
RQQ					
0052+251	0.154	15.9	-23.9	21.55	700±478
0054+144	0.171	15.7	-24.3	21.87	-115±138
0157+001	0.164	15.7	-24.2	22.87	138±280
0204+292	0.109	16.0	-23.0		675±524
0205+024	0.155	15.4	-24.5		173±299
0244+194	0.176	16.7	-23.4	21.30	-123±140
0257+024	0.115	16.1	-23.0	22.19	-53±112
0316-346	0.265	15.1	-26.0		227±336
0923+201	0.190	15.8	-24.4	21.26	930±501
0953+414	0.239	15.6	-25.3	21.71	1359±553
1012+008	0.185	15.9	-24.3	22.00	737±459
1029-140	0.086	13.9	-24.7		448±489
1116+215	0.177	14.7	-25.5		598±438
1202+281	0.165	15.6	-24.5		955±547
1307+085	0.155	15.1	-24.8		209±327
1309+355	0.184	15.6	-24.7		-134±143
1402+261	0.164	15.5	-24.5		-106±135
1444+407	0.267	15.7	-25.4		-107±241
1635+119	0.146	16.5	-23.1	23.02	182±300
2215-037	0.241	17.2	-23.7	21.43	-52±241
2344+184	0.138	15.9	-23.6	21.11	209±314

Table 3. Sample details and spatial clustering results. Column 5 details the 5GHz radio luminosity (where known) in units of $\text{Whz}^{-1}\text{sr}^{-1}$. The errors have been calculated using the conservative prescription of Yee & López-Cruz (1999): $\frac{\Delta B_{gq}}{B_{gq}} = \frac{[(N_t - N_b) + 1.3^2 N_b]^{1/2}}{N_t - N_b}$

& Peacock 1988, Andersen & Owen 1994). Evidence that the calibration proposed here is also reasonable for the very richest clusters comes from the fact that the four richest clusters studied by Yee & López-Cruz had a mean value of $B_{gq} = 2225$ Mpc^{1.77}, here corresponding to Abell class 4/5, with no clusters found with $B_{gq} > 2300$ Mpc^{1.77}. It can be

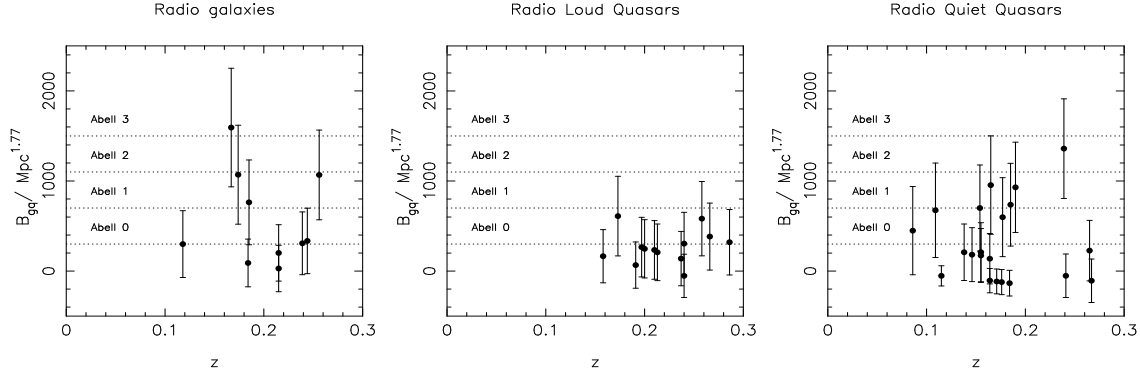


Figure 5. The $B_{gq} - z$ distribution for the three sub-samples. Also shown are the approximate Abell cluster classifications according to the linear scheme shown in Table 4.

Abell Class	0	1	2	3	4	5
B_{gq}	300	700	1100	1500	1900	2300

Table 4. The proposed relation between spatial clustering amplitude and Abell classification. This scheme is identical to that proposed by Yee & López-Cruz (1999) but with Abell Class 0 clusters normalized to $B_{gq} = 300$ instead of $700 \text{ Mpc}^{1.77}$ (see text)

seen that using our calibration of the B_{gq} –Abell transformation the results presented in this section imply that the average clustering around our AGN corresponds to Abell class $\simeq 0$, with the large scatter ranging from several objects consistent with no galaxy enhancement, to several clusters of Abell class 2/3.

5 DO THE ENVIRONMENTS OF RADIO-LOUD AGN CHANGE AT $Z=0.5$?

The clustering results for the radio galaxy and radio-loud quasars sub-samples presented in the previous section offer an opportunity to re-examine the evidence for an epoch-dependent change in cluster richness at $z \sim 0.5$. In this section we investigate this issue by comparing our results with those published for radio galaxies by Hill & Lilly (1991) and the recent work on radio-loud quasars by Wold et al. (2000a).

5.1 Radio galaxies

In their study of the environments of radio galaxies Hill & Lilly (1991) studied four groups of $\simeq 10$ objects at $z \simeq 0.5$, each of which were equally spaced in radio power from $\text{Log } P_{2GH_z} = 23 \rightarrow 27 \text{ WHz}^{-1}$. To compare their results with those for our radio galaxy sample we selected objects from their two medium radio luminosity groups, subject to the redshift constraint $0.40 < z < 0.53$, which was chosen to match the range in redshift displayed by our radio galaxies ($0.12 < z < 0.26$). This selection procedure produced 16 objects, two of which were quasars and subsequently rejected to leave a final sample of 14 objects. The $P_{2GH_z} - M_B$ and $P_{2GH_z} - z$ distributions of the Hill & Lilly sub-sample and

our radio galaxy sample are shown in the left and middle panels of Fig 6. The two samples are clearly well matched, with the two-dimensional KS test (2DKS) showing their respective $P_{2GH_z} - M_B$ distributions to be statistically indistinguishable ($p = 0.2$).

To facilitate a comparison between the cluster richness determinations of Hill & Lilly and our own results it was necessary to transform between B_{gq} and their $N_{0.5}$ values. The value of $N_{0.5}$ is the background subtracted number of galaxies within a radius of 0.5 Mpc, in the magnitude range $m_g \rightarrow m_g + 3$, where m_g is the apparent magnitude of the radio galaxy. As previously mentioned in Section 3, this magnitude range should be well matched to our choice of $m_* - 1 \rightarrow m_* + 2$, and to make the transformation we have used Hill & Lilly’s own determination of $B_{gq} = 30N_{0.5}$. The resulting $B_{gq} - z$ distributions for the two samples are shown in the right-hand panel of Fig 6. It can be seen that the two distributions are very similar, an impression confirmed by a KS test ($p = 0.77$), with no indication that the members of the low- z sample inhabit poorer environments, or that they display a smaller range in environment richness. Although we are dealing with small samples, this result demonstrates that, at least for these two well matched samples, there appears little evidence for a epoch-dependent change in FR II radio galaxy environments at $z \simeq 0.5$. In light of this, we now move on to look for a change in the environments of radio-loud quasars with redshift.

5.2 Radio-loud quasars

The recently published study of 21 RLQs in the redshift interval $0.5 < z < 0.8$ by Wold et al. (2000a) provides a good opportunity for comparison with the results from our $z \simeq 0.2$ RLQ sample. Wold et al. also classify the environments of their quasars via the spatial clustering amplitude and their results can therefore be directly compared to our own. Taken as a whole the results for their sample are in excellent agreement with our own, with their mean figure of $B_{gq} = 265 \pm 65 \text{ Mpc}^{1.77}$ being almost identical to our mean of $B_{gq} = 267 \pm 51 \text{ Mpc}^{1.77}$.

To disentangle the effects of redshift and radio luminosity we have excluded the 7 most radio luminous of the Wold et al. sample ($\text{Log } P_{408} > 26.5 \text{ WHz}^{-1} \text{sr}^{-1}$) to leave a sub-sample of 14 objects which are well matched to our 12-object RLQ sample. The distribution of the two samples on

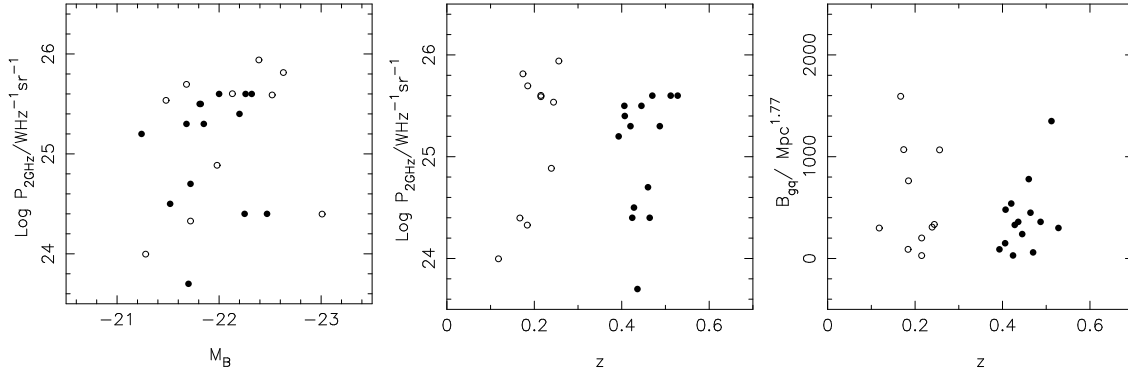


Figure 6. The left-hand and middle panels show the matching of our RG sample (open circles) with the sub-sample of the objects studied by Hill & Lilly (1991) discussed in the text (filled circles). The right-hand panel shows a comparison between their respective spatial clustering amplitudes.

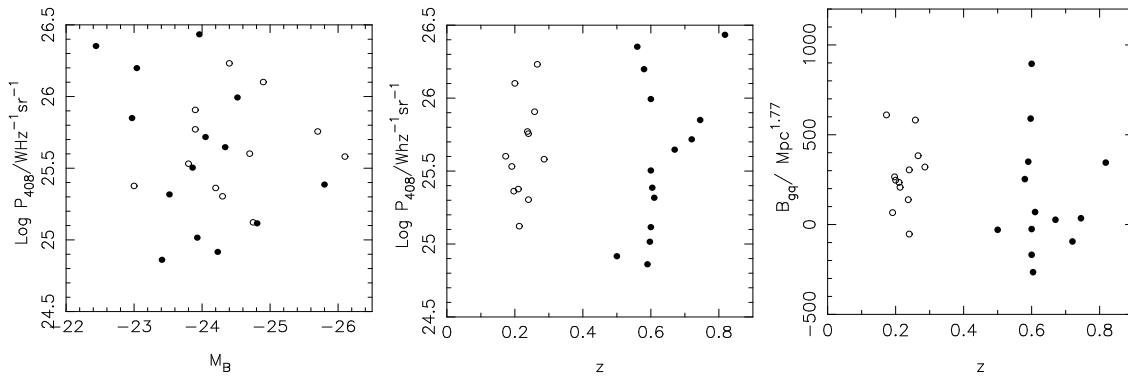


Figure 7. The left-hand and middle panels show the matching between our RLQ sample (open circles) and the sub-sample of the objects studied by Wold et al. (2000a) discussed in the text (filled circles). The right-hand panel shows a comparison of their respective spatial clustering amplitudes.

the $P_{408}-M_B$ and $P_{408}-z$ planes is shown in the left-hand and middle panels of Fig 7. The two samples can be seen to be well matched, with the 2DKS test returning a probability of $p = 0.51$ that the two samples are drawn from the same $P_{408}-M_B$ distribution. From the comparison of the spatial clustering amplitudes of the two samples shown in the right-hand panel of Fig 7, there is again no suggestion that the high- z sample displays systematically higher values of B_{gq} , although it is noticeable that the scatter in B_{gq} is somewhat higher in the high- z sample. This is in fact the conclusion arrived at by Wold et al., who also found no evidence for an epoch-dependent change in RLQ environments when comparing their results with those of Ellingson, Yee & Green (1991) at low redshift.

6 EVIDENCE FOR A LINK BETWEEN AGN PROPERTIES AND HOST CLUSTER ENVIRONMENT

In this section we explore whether there is any evidence in our data for a link between AGN properties and the large-scale environments of their hosts. This issue is of interest because it offers the potential to determine whether the radio and optical luminosity of powerful AGN are primarily influenced by large-scale environmental factors such as den-

sity of the ICM and galaxy interactions, or alternatively, whether the physical properties of the active nucleus itself, such as black-hole mass and accretion rate, are the dominant influence.

The three panels shown in Fig 8 display the relationship between B_{gq} and respectively, estimated central black-hole mass, quasar accretion efficiency and radio luminosity. All three panels feature only those objects from the sample imaged in the McLure et al. (1999), and Dunlop et al. (2000) host-galaxy study in order to produce a homogeneous dataset. The objects from the Bahcall et al. (1997) sample have been excluded on the basis that, due to the saturated nature of their data, reliable nuclear luminosities are unavailable.

In the left-hand panel of Fig 8 we have plotted B_{gq} against black-hole mass, as calculated by a straight application of the galaxy bulge mass-blackhole mass relation published by Magorrian et al. (1998) to the host galaxy modelling results presented in Dunlop et al. (2000). A general trend for black-hole mass to increase with spatial clustering amplitude can be seen, although the correlation is not statistically significant, with a Spearman rank test returning a probability of $p = 0.38$ of no correlation. The clearest signal comes from the ten radio galaxies, although even here Kendall's tau test still returns only a marginally significant result; $p = 0.09$. However, the lack of a clear correlation between B_{gq} and black-hole mass is perhaps not entirely

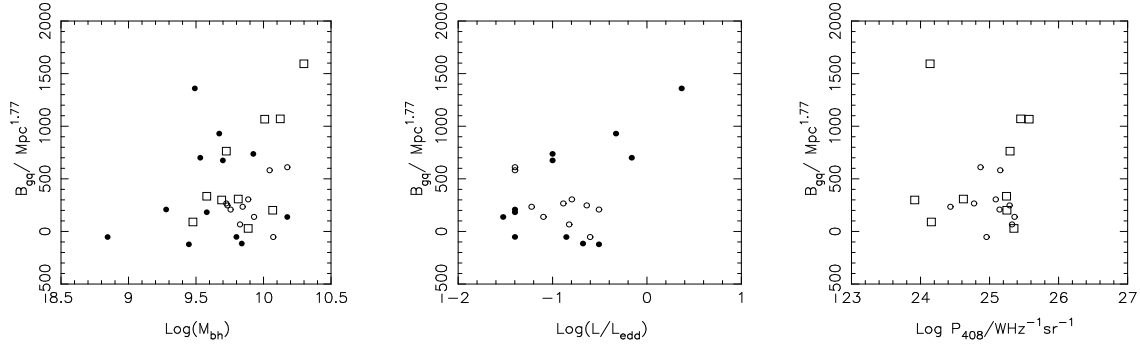


Figure 8. Plots of the B_{gq} versus black-hole mass (left), quasar nuclear luminosity as a fraction of the Eddington limit (middle) and radio luminosity at 408MHz (right). In all three plots RQQs are represented by filled circles, RLQs are represented by open circles and RGs are represented by open squares.

unexpected. Even if the basic form of the cluster luminosity function does not change significantly with cluster richness, there will be a corresponding increase in the number of luminous, bulge-dominated galaxies which are capable of hosting powerful AGN as cluster richness increases. Consequently, in rich clusters, it is not only the central brightest-cluster galaxy which is a potential AGN host, but also the next few lower-ranked cluster galaxies. This then will inevitably introduce significant horizontal scatter into the B_{gq} -blackhole mass relation, regardless of the 0.5 dex scatter in the Magorrian relation itself.

The middle panel of Fig 8 shows the relationship between B_{gq} and the nuclear luminosity of the quasars, expressed as a fraction of their Eddington limit, under the assumption of a central black-hole mass as predicted by the Magorrian relation. As with the previous plot, a trend can be seen for the Eddington fraction to increase with cluster richness, although again this is not statistically significant, with a rank test returning a probability of $p = 0.5$ that no correlation is present. However, it is perhaps interesting to note that the three RQQs which are radiating closest to their predicted Eddington limit are also ranked first, second and fourth in terms of their cluster richness.

Finally, the right-hand panel of Fig 8 examines whether there is a correlation between the radio luminosity of the radio-loud AGN in our sample, and the density of the environment into which their radio jets are expanding. As with the other two plots in Fig 8 a positive correlation is again suggested to the eye, but is once more found not to be significant, with a rank test returning a probability of $p = 0.47$ of no correlation, even after the removal of the obvious outlying radio galaxy. It is also noteworthy that the apparent positive trend between radio luminosity and B_{gq} is entirely defined by the ten radio galaxies, with the RLQs showing no evidence for a connection between radio luminosity and cluster richness. Consequently, at least for this sample of objects, there appears no real evidence that the density of a radio-loud AGN's cluster environment plays the dominant role in determining its radio luminosity. However, it is also clear that the limited dynamic range of this sample, combined with the inherently large uncertainties associated with spatial clustering amplitudes, means that the results presented here are still perfectly consistent with a weak correlation being present.

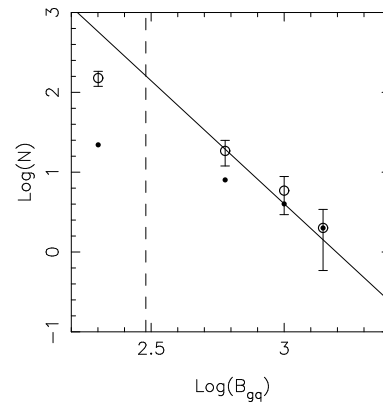


Figure 9. A comparison between our AGN cluster number counts with those of the APM cluster survey using a bin size of $\Delta B_{gq} = 400$. The solid circles are our uncorrected number counts, while the open circles are weighted using the inverse of the mean B_{gq} in each bin (see text). The solid line is a power-law with slope -3.7 which fits the APM number counts and has arbitrary vertical normalization. The vertical dotted line indicates where the APM survey becomes incomplete.

7 COMPARING AGN ENVIRONMENTS TO THE APM CLUSTER SURVEY

In Section 5 it was shown that with samples of RQQs and RLQs which are carefully matched in terms of optical luminosity there is no evidence that RQQs occupy systematically lower-density cluster environments. This result therefore makes it of interest to re-examine the question of whether quasars actually avoid rich clusters, as sometimes claimed, or if alternatively the apparent lack of quasars in rich clusters is simply a reflection of the fact that rich clusters are relatively scarce.

In order to address this question we have compared our cluster results with cluster number counts from the APM survey, which are well modelled by a power-law with slope $\simeq -3.7$ (Dalton et al. 1997). To allow a fair comparison of the relative numbers of clusters it is necessary to correct for the fact that the number of potential AGN host galaxies increases with cluster richness. To allow for this effect we make the assumption that the galaxy population of all our clusters can be described by a Schechter function with constant characteristic magnitude and faint-end slope, and a normal-

ization simply proportional to B_{gq} . Consequently, in Fig 9 we have simply weighted the relative number counts of clusters by the inverse of the mean B_{gq} in each bin. As can be seen in Fig 9 this simple correction naturally produces number counts which are perfectly consistent with the power-law found by the APM survey.

A further interesting result arises if one considers the space densities of clusters from the APM survey as calculated by Croft et al. (1997). With the calibration that in the scheme used in the analysis of the APM survey, a cluster of richness $R=40$ corresponds to roughly Abell class 0 (ie. $B_{gq} \sim 300 \text{ Mpc}^{1.77}$), it is possible to extrapolate the figures provided by Croft et al. to estimate that the space density of all clusters richer than $R \geq 40$ is $\simeq 10^{-5} \text{ Mpc}^{-3}$. If one allows for the fact that up to 50% of quasars could be obscured in the optical-UV by a dusty torus, this abundance of clusters is in reasonable agreement with the peak space density of quasars at $z \sim 2.5$ (Warren, Hewett & Osmer 1994).

This line of argument leads to an interesting conclusion concerning the fraction of massive cluster galaxies which were active at $z \sim 2.5$. In their photometric study of 83 Abell clusters Schneider, Gunn & Hoessel (1983) determined the absolute magnitudes of the three brightest galaxies in each cluster. When converted to our cosmology, the mean magnitude of the first ranked galaxy in clusters of Abell class 0 corresponds to $M_R \simeq -23.1 \pm 0.5$, where a colour of $r - R = 0.35$ has been assumed (Fukugita et al. 1995). This is in excellent agreement with the figure of $M_R \sim -23$ which was found to be the necessary bulge luminosity for a galaxy to host a powerful ($M_V < -23$) quasar by Dunlop et al. (2000). Furthermore, because the mean luminosity found by Schneider, Gunn & Hoessel for the second ranked galaxy in Abell class 0 clusters was approximately one magnitude fainter than that of the first ranked galaxies, we can conclude that the average number of massive elliptical galaxies in a Abell class 0 cluster which are capable of hosting a powerful quasar is close to unity. Consequently, because of the steep decline in the number of clusters with increasing richness (Fig 9), the close agreement between the peak space density of quasars and that of clusters of Abell class ≥ 0 leads to the conclusion that virtually all massive cluster ellipticals were active at $z \sim 2.5$. This conclusion is unaffected by the fact that the very richest clusters may have contained 4 or 5 active galaxies at this epoch because the rarity of such clusters means that they have a negligible affect on quasar numbers.

8 CONCLUSIONS

The cluster environments of a matched sample of 44 powerful radio-loud and radio-quiet AGN at $z \sim 0.2$ have been analysed using the spatial clustering amplitude method. The three main conclusions arising from this study can be summarized as follows:

Firstly, we find no evidence to suggest that RQQs inhabit poorer cluster environments than RLQs or RGs. All three classes of AGN are located in environments which, on average, are comparable to Abell Class 0, although there is a large amount of scatter.

Secondly, by comparing our results with those for samples from Hill & Lilly (1991) and Wold et al. (2000a)

which are matched in terms of redshift and radio luminosity, we have re-examined the evidence for an epoch-dependent change in the environments of RLQs and RGs. We find no evidence that the environments of RGs and RLQs become significantly richer at $z \simeq 0.5$ as has been reported by Hill & Lilly (1991) and Ellingson, Yee & Green (1991) respectively.

Finally, via comparison with the APM cluster survey we conclude that the distribution of AGN cluster environments is consistent with having being drawn at random from the general cluster distribution. Furthermore, because the cluster population is dominated by clusters of Abell class $\simeq 0$ which, on average, only contain one galaxy capable of hosting a powerful quasar, we argue that the close agreement between the space density of clusters and the peak space density of quasars at $z \sim 2.5$ suggests that practically all massive cluster ellipticals were active at this epoch. In this scenario, the apparent lack of powerful AGN in rich clusters at the present day simply reflects the comparative scarcity of high density environments.

9 ACKNOWLEDGEMENTS

Based on observations with the NASA/ESA Hubble Space Telescope, obtained at the Space Telescope Science Institute, which is operated by the Association of Universities for Research in Astronomy, Inc. under NASA contract No. NAS5-26555. This research has made use of the NASA/IPAC Extragalactic Database (NED) which is operated by the Jet Propulsion Laboratory, California Institute of Technology, under contract with the National Aeronautics and Space Administration. The authors thank Philip Best and Lance Miller for their useful comments. RJM acknowledges a PPARC PDF.

10 REFERENCES

- Abell G., 1958, ApJS, 3, 211
- Abell G., Corwin H.G., Olowin R.P., 1989, ApJS, 70, 1
- Andersen V., Owen F.N., 1994, AJ, 108, 361
- Bahcall J.N., Kirhakos S., Saxe D.H., Schneider D.P., 1997, ApJ, 479, 642
- Best P.N., Longair M.S., Röttgering H.J.A., 1997, MNRAS, 292, 758
- Best P.N., Longair M.S., Röttgering H.J.A., 1998, MNRAS, 295, 549
- Boyce P.J., et al., 1998, MNRAS, 298, 121
- Croft R.A.C., Dalton G.B., Efstathiou G., Sutherland W.J., Maddox S.J. 1997, MNRAS, 291, 305
- De Robertis M.M., Hayhoe K., Yee H.K.C., 1998, ApJS, 115, 163
- Dalton G.B., Maddox S.J., Sutherland W.J., Efstathiou G., 1997, MNRAS, 289, 263
- Dunlop J.S., et al., 1993, MNRAS, 264, 455
- Dunlop J.S., et al., 2000, MNRAS, in prep
- Ellingson E., Yee H.K.C., Green R.F., 1991, ApJ, 371, 49
- Fisher K.B., Bahcall J.N., Kirhakos S., 1996, ApJ, 468, 468
- Fukugita M., Shimasaku K., Ichikawa T., 1995, PASP 107, 945
- Groth E.J., Peebles P.J.E., 1977, ApJ, 217, 385
- Hall P.B., Green R.F., 1998, ApJ, 507, 558

- Hill G.J., Lilly S.J., 1991, ApJ, 367, 1
Holtzman J.A., et al., 1995, PASP, 107, 1065
Hooper E.J., Impey C., Foltz C.B., 1997, ApJ, L95
Laing R.A., Riley J.M., Longair M.S., 1983, MNRAS, 204, 151
Lilly S.J., Prestage R.M., 1987, MNRAS, 225, 531
Lilly S.J., et al., 1995, ApJ, 455, 108
Longair M.S., Seldner M., 1979, MNRAS, 189, 433
Loveday J., Peterson B.A., Efstathiou G., Maddox S.J., 1992, ApJ, 390, L338
Magorrian J., et al., 1998, AJ, 115, 2285
McLure R.J., et al., 1999, MNRAS, 308,377
Metcalf N., Shanks T., Fong R., Jones L.R., 1991, MNRAS, 249, 498
Prestage R.M., Peacock J.A., 1988, MNRAS, 230, 131
Prestage R.M., Peacock J.A., 1989, MNRAS, 236, 959
Schade D.J., Boyle B.J., Letawsky M., 2000, MNRAS, 315, 498
Schneider D.P., Gunn J.E., Hoessel J.G., 1983, ApJ, 268, 476
Smith E.P., O'Dea C.P., Baum S.A., 1995, ApJ, 441, 113
Smith R.J., Boyle B.J., Maddox S.J., 1995, MNRAS, 277, 270
Smith R.J., Boyle B.J., Maddox S.J., 2000, MNRAS, 313, 252
Stoche J.T., et al., 1983, ApJ, 273, 458
Taylor G.L., et al., 1996, MNRAS, 283, 930
Warren S.J., Hewett P.C., Osmer P.S., 1994, ApJ, 421, 412
Wold M., Lacy M., Lilje P.B., Serjeant S., 2000a, MNRAS, submitted (astro-ph/9912070)
Wold M., Lacy M., Lilje P.B., Serjeant S., 2000b, (astro-ph/0006063)
Wurtz R., Stoche J.T., Ellingson E., Yee H.K.C., 1997, ApJ, 480, 547
Yates M.G., Miller L., Peacock J.A., 1989, MNRAS, 240, 129
Yee H.K.C., Green R.F., 1984, ApJ, 280, 79
Yee H.K.C., Green R.F., 1987, ApJ, 319, 28
Yee H.K.C., Ellingson E., 1993, ApJ, 411, 43
Yee H.K.C., López-Cruz O., 1999, AJ, 117, 1985